

A novel method for telescope polarization modeling based on an artificial neural network

Jian-Guo Peng^{1,2}, Shu Yuan^{1*}, Kai-Fan Ji¹ and Zhi Xu¹

¹ Yunnan Observatories, Chinese Academy of Sciences, Kunming 650216, China; yuanshu@ynao.ac.cn

² University of Chinese Academy of Sciences, Beijing 100049, China

Received 2020 December 22; accepted 2021 February 2

Abstract The polarization characteristics of an astronomical telescope is an important factor that affects polarimetry accuracy. Polarization modeling is an essential means to achieve high precision and efficient polarization measurement of the telescope, especially for the alt-azimuth mount telescope. At present, the polarization model for the telescope (i.e., the physical parametric model) is mainly constructed using the polarization parameters of each optical element. In this paper, an artificial neural network (ANN) is used to model the polarization characteristics of the telescope. The ANN model between the physical parametric model residual and the pointing direction of the telescope is obtained, which reduces the model deviation caused by the incompleteness of the physical parametric model. Compared with the physical parametric model, the model fitting and predictive accuracy of the New Vacuum Solar Telescope (NVST) is improved after adopting the ANN model. After using the ANN model, the polarization cross-talk from I to Q, U, and V can be reduced from 0.011 to 0.007, and the crosstalk among Q, U, and V can be reduced from 0.047 to 0.020, which effectively improves the polarization measurement accuracy of the telescope.

Key words: techniques: polarimetric — telescopes — polarization — instrumentation: polarimeters

1 INTRODUCTION

The solar magnetic field plays a critical role in solar activity, and the corresponding observed data is of great importance to study the mechanism of solar activity (Yan et al. 2018; Xue et al. 2020). At present, the solar magnetic field is mainly derived by the spectropolarimetric measurement of observational targets based on the Zeeman effect, and the polarization effect of the solar telescope is supposed to be removed from polarization observations (Skumanich et al. 1997; Beck et al. 2005a,b; Ichimoto et al. 2008; Schou et al. 2012; Hofmann et al. 2012; Anan et al. 2018; Ahn & Cao 2019; Hou et al. 2020; Harrington et al. 2019). Thus, we need to measure the polarization property of solar telescope with polarimetric instruments, and the conventional method for the polarization calibration of the telescope is installing an instrumental polarization calibration unit (ICU), which usually consists of a polarizer and a retarder, in the front of the relay optics or the whole telescope to measure the Mueller matrix of the telescope.

For example, the German Vacuum Tower Telescope (VTT) on Tenerife (Beck et al. 2005a,b), the Solar Optical telescope (SOT) onboard Hinode (Ichimoto et al. 2008), the Helioseismic and Magnetic Imager (HMI) aboard the Solar Dynamics Observatory (SDO) (Schou et al. 2012), the GREGOR solar telescope (Hofmann et al. 2012), the New Solar Telescope (NST) at Big Bear Solar Observatory (Ahn & Cao 2019), the New Vacuum Solar Telescope (NVST) (Wang et al. 2013; Liu et al. 2014; Hou et al. 2020), the Daniel K. Inouye Solar Telescope (DKIST) (Harrington et al. 2019) and the future European Solar Telescope (EST) (Bettonvil et al. 2010). Since there is no relative rotation of optical elements while the space telescope or ground-based telescope without relay optics points to the target, the polarization property of these telescopes remains constant with time if we do not consider the degenerate of mirror coatings (Ichimoto et al. 2008; Schou et al. 2012). In comparison, the large aperture ground-based telescopes are usually installed on an alt-azimuth mount, and consist of relay optics to convey the light to the Coude laboratory, where the focal

* Corresponding author

plane is stationary and more instruments can be added (Hofmann et al. 2012; Hou et al. 2020; Ahn & Cao 2019; Harrington et al. 2019). This leads to the time-dependent incidence angles on optical elements along the light path to the optical laboratory. Thus, the polarization property of the telescope and focal instruments is time-varying and depends on the pointing direction of the telescope (Skumanich et al. 1997; Beck et al. 2005b; Yuan 2014, 2019; Liu et al. 2015).

The polarization calibration for the space telescope or ground telescope without relay optics is relatively simple since there is no need to consider the pointing direction of the telescope, and the calibration result can be directly used for the correction of polarimetric observations. It is more complicated to calibrate the polarization property of a ground-based solar telescope with relay optics, and we cannot directly use the calibration result to correct the observed data since the polarization property changes over time. Therefore, it is essential to construct a polarization model, the relationship between the polarization property and time (or pointing direction) of the telescope, for a ground-based telescope with relay optics.

Polarization modeling for the large-aperture ground telescope is a complex problem with multiple factors, such as the polarization characteristics of each mirror, the relative rotation between the mirror groups, the alignment error between the mirror groups, and the model error of mirrors. Besides, some telescopes have vacuum windows, and their polarization characteristics are difficult to describe with a simple model. Therefore, the polarization model based on the ideal optical system assumption, which is referred to below as the physical parametric model, can include the main polarization characteristics of the telescope, but it is difficult to take all the polarization factors into account. The parameters of the physical parametric model are obtained by fitting the polarization calibration data and the measured Mueller matrix of the telescope. The maximum deviation of the polarization calibration data from the physical parametric model of the telescope varies with telescopes and ranges from 0.04 to 0.08 (Anan et al. 2018; Ahn & Cao 2019; Yuan 2019). Thus the accuracy of the parametric model needs to be improved since the requirement of the model accuracy is much higher than the previous deviation. It is difficult to improve the model accuracy of the physical parametric model because the source of the model deviation cannot be determined.

With the development of observational technology in astronomy, the amount of astronomical data continues to increase, which also makes it more difficult for

astronomers to process and analyze data. Machine learning has developed rapidly in recent years and was used to deal with problems in astronomy and astrophysics. With its advantages in the recognition and extraction of image structures, the analysis of the implicit correlation of complex data, and the classification of data, machine learning has shown great potential in handling astronomical tasks, such as gravitational wave detection, searching for exoplanets, classification of galaxies and spectra, prediction of solar flares, calibration of solar magnetographs (Baron 2019; George & Huerta 2018; Pearson et al. 2018; Kim & Brunner 2017; Huang et al. 2018; Hála 2014; Hao et al. 2018; Guo et al. 2020). The previous research based on machine learning also inspires us to use this approach to tackle new issues, which are suitable for machine learning and cannot be well addressed by conventional methods.

Telescope polarization modeling is such a problem that it is suitable for machine learning owing to its great capacity of fitting, and has not been properly solved by the physical parametric model since the fitting and predictive accuracy is insufficient. Thus, we utilize machine learning to establish the relationship between the Mueller matrix of the telescope, which can describe the polarization property of the telescope, and the pointing direction of the telescope (represented by the altitude and azimuth angle of the telescope). In this article, we take the New Vacuum Solar Telescope (NVST) as an example and derive the polarization model of the telescope based on machine learning — ANN to be exact. The artificial neural network (ANN) polarization model can provide more accurate fitting and predicting of the Mueller matrix of the telescope, and output the Mueller matrix of the telescope according to the time or pointing direction. The accuracy of the ANN polarization model is about 0.02 in all Mueller matrix elements, and higher than 0.007 for the first column, which requires higher accuracy in modeling. The ANN polarization model for NVST meets the requirements of the telescope polarization modeling.

Section 2 contains the description of the optical configuration of NVST, the polarization characteristics of the telescope's optical system, and the results of the physical parametric model. The structure and hyperparameters of the ANN polarization model are described in Section 3. The training results of the ANN polarization model and the model predictive performance are presented in Section 4. The conclusions and discussions are given in Section 5.

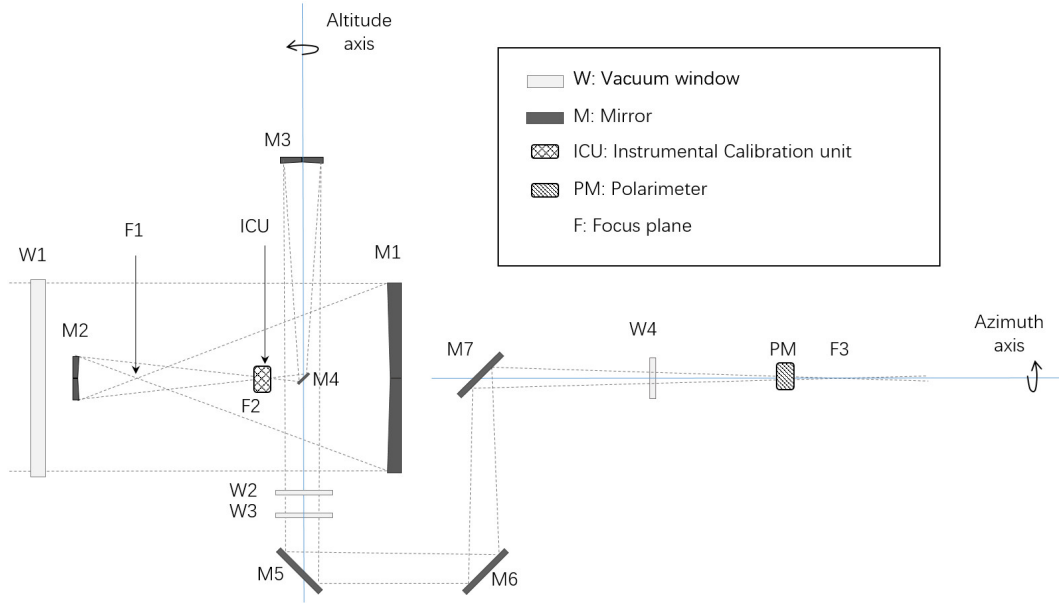


Fig. 1 The schematic of NVST optical configuration.

2 THE POLARIZATION PROPERTY OF THE NVST

Figure 1 shows the optical configuration of the NVST, the labels with M represent mirrors, the labels with W mean vacuum windows, and the label F means focal plane. The sunlight entering the solar telescope from vacuum window W1 is reflected by or transmitted through M1, M2, M4, M3, W2, W3, M5, M6, M7, W4 and then enters the Coude laboratory; the focal plane F3 is the Coude focal plane. An ICU, which can generate a known polarization state with a rotating polarizer and a rotating retarder, is mounted near the focal plane F2 after the secondary mirror M2 of the telescope to calibrate the polarization characteristics of optical elements after M2. A polarimeter, which consists of a rotating retarder and a fixed polarization analyzer, is installed near the focal plane F3 to implement polarimetry. The polarimeter is followed by a multi-wavelength spectrograph and a high-resolution magnetograph, both of which are designed to achieve polarimetric observation of the photospheric line Fe I 532.4 nm. The polarization calibration data are obtained by the spectrograph with a polarimeter at 532.4 nm, in order to separate the polarization property of the telescope from the polarimetric observations. Based on the polarization calibration data, we can build up the polarization model of the telescope. The primary aim of this paper is to validate the practicability of telescope polarization modeling based on machine learning, the detailed parameters of the ICU, the polarimeter, and the processing of the polarization

calibration data is to be found in the work of Hou et al. (2020).

A previous study by Yuan (2014) has reported that the polarization effect, described by the Mueller matrix, introduced by the telescope’s primary and secondary mirror is at the level of 10^{-5} , which is much smaller than the noise level (10^{-3}) of the polarimetric instrument. In addition, it has been demonstrated that the main vacuum window’s polarization characteristics of the NVST are negligible, smaller than 10^{-2} , and only introduce crosstalk between the circular polarization and linear polarization, for most of the observational time in the article Liu et al. (2015). Therefore, the polarization property, specifically the Mueller matrix, measured by the ICU and polarimeter can represent the polarization characteristics of the whole telescope. As shown in Figure 1, there are four mirrors (M4, M5, M6, and M7) with an incident angle of 45° in the relay optics of the telescope, and each mirror can produce considerable polarization due to the large incident angle. In addition, M5, M6, and M7 share the same incident plane, which means the polarization effect of the three mirrors has to be added up, so the NVST has a strong instrumental polarization. The azimuth angle of the telescope changes rapidly at noon near the summer solstice, which can cause a rapid change of the Mueller matrix of the telescope since the geographic location of NVST (longitude= $102^\circ 57' 11''$, latitude= $24^\circ 34' 47''$) is in the vicinity of the Tropic of Cancer. The polarization effects of the vacuum windows (W2, W3, and W4) in the optical path are uncharted. These factors all add to the complexity of polarization calibration and polarization modeling of the telescope.

Thus, the present physical parametric model of NVST cannot describe the polarization characteristics of NVST well.

In previous literature Yuan (2014, 2019), a physical parametric model for the NVST was built up and the parameters were derived after the model fitting. Figure 2 provides the measured and simulated Mueller matrix profile of NVST at different universal times on 2019 April 24, and the difference between them. Each subgraph corresponds to the element of the 4×4 Mueller matrix, and there is no apparent discrepancy between the measured and simulated Mueller matrix in Figure 2(a), indicating that the physical parametric model can describe the main polarization characteristics of the NVST. It can be seen from Figure 2(a) that the M_{23} , M_{24} , M_{32} , M_{34} , M_{42} , and M_{43} elements have values close to 1 or -1 , suggesting that the polarization effect of the telescope is significant and can cause serious crosstalk between Q, U, and V signals. Furthermore, these Mueller matrix elements change drastically over time, especially the M_{23} , M_{24} , M_{32} , and M_{34} . Therefore, the polarization model, which can characterize the polarization effect of the telescope, is of great significance to improve the efficiency and accuracy of the polarimetric instruments.

Even though the physical parametric model coincides with the measured Mueller matrix in Figure 2(a), the differences between them are not ignorable in Figure 2(b) and are systematical over time. For example, the maximum residual error of the M_{32} element is about 4%, which means that there remains a maximum of 4% crosstalk from Q to U after calibration by the physical parametric model. The maximum systematic residual errors of M_{21} and M_{31} are about 1%, which need to be handled carefully since the I signal is usually dozens of times larger than the Q, U, and V signals in solar observation. The deviation between the present physical model and measured Mueller matrix of other days is at the same level of Figure 2 and has different tendencies over universal time. Thus, the polarization model requires improvement while the noise level is about 3×10^{-3} of the intensity in the continuous spectrum.

Based on the present physical model and the pointing direction of the telescope, the rate of the Mueller matrix change in different months and observational times can be acquired. In the months around the summer solstice, the Mueller matrix of the telescope changes greatly with time at noon because of the drastic change of the azimuth angle. The measured Mueller matrix of the telescope would deviate from the actual value at the corresponding time owing to the duration of the calibration measurement,

which also needs to be considered in the subsequent data processing.

3 THE STRUCTURE OF THE MACHINE LEARNING MODEL

Due to the complexity of the polarization characteristics of the NVST, the physical parametric model cannot fully describe the relationship between the Mueller matrix and the pointing direction (i.e., the altitude and azimuth angle) of the telescope. Therefore machine learning, specifically the ANN, is adopted to construct the polarization model of the telescope. Take advantage of ANN's performance in regression, the ANN model can be used to describe the intricate nonlinear relationship between the input data and the target value (Baron 2019).

Since the physical parametric model includes the principal polarization characteristics of the telescope, the residual of the physical parametric model is set as the target value while the altitude and azimuth angle of the telescope is the input data. Because the first element of the Mueller matrix residual is 0, the other 15 elements are used as the target value during machine learning training. The ANN model here is used to establish the relationship between the residual of the physical parametric model and the altitude and azimuth angle. After the ANN model is derived, the combination of the physical parametric model and the ANN model can be used to describe the polarization property of the telescope, and the Mueller matrix of the telescope can be obtained according to the altitude and azimuth angle of the telescope.

Figure 3(a) shows the basic structure of the ANN model used in this article, including an input layer, a hidden layer, and an output layer. The neurons of the hidden layer are fully connected to the neurons of the input and the output layer. The structure of each neuron is shown in Figure 3(b) and the activation function used in the hidden layer is the sigmoid function. In Figure 3(a), Azi and Alt in the input layer is the azimuth and altitude angle of the telescope, and ΔM_{ij} in the output layer corresponds to the element of the Mueller matrix residual. The hidden layer here only consists of a single layer with 20 neurons, since more neurons or layers can increase the possibility of overfitting, and the predictive accuracy of the ANN model would even decrease.

The Bayesian regularization algorithm is adopted in the training process, and the mean square error (MSE) is used as the loss function. The main parameters are displayed in Table 1, which are selected according to the fitting and predictive performance.

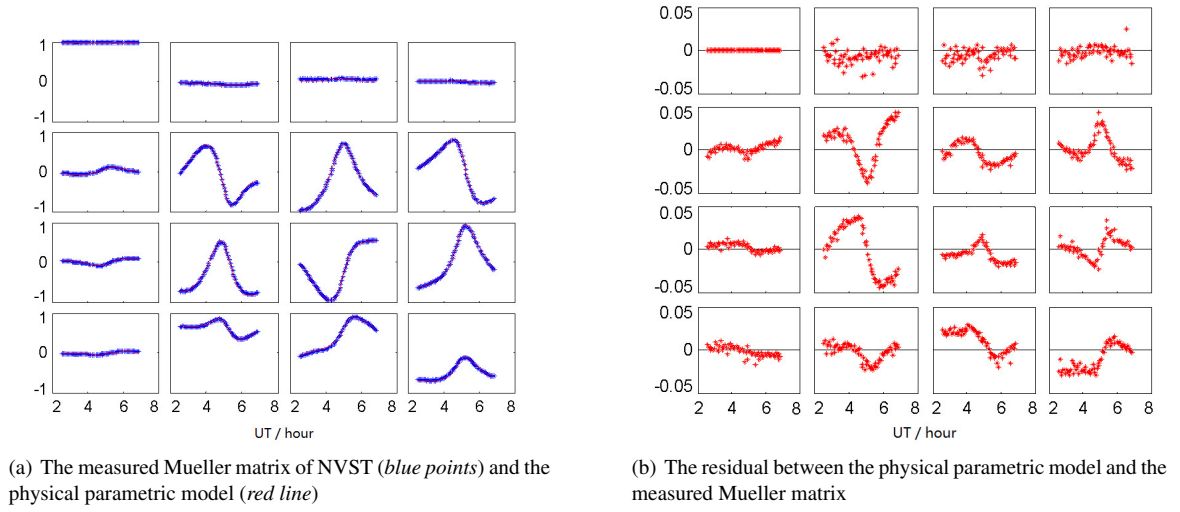


Fig. 2 Comparison of the measured Mueller matrix and the physical parametric model on 2019 April 24.

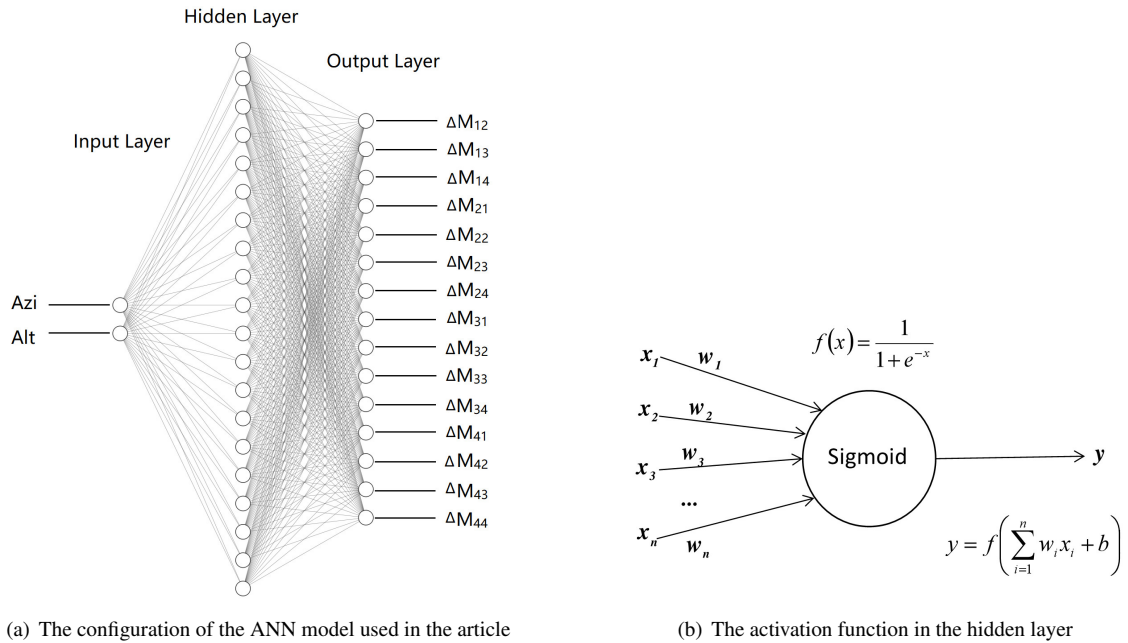


Fig. 3 The artificial neural network (ANN) model.

Table 1 The Main Parameters of the ANN Model

Parameters	Value	Description
Max_epochs	1000	Maximum number of epochs to train
Train_ratio	70%	Ratio of training data
Val_ratio	15%	Ratio of validation data
Test_ratio	15%	Ratio of testing data
Max_fail	30	Maximum number of validation failures
Min_grad	10^{-10}	Minimum gradient of performance
Goal	6×10^{-6}	Goal for performance
Learn_rate	0.001	Learning rate

4 RESULTS

4.1 Data Preprocessing

Since the ANN model is derived from the polarization calibration data, the data preprocessing is a significant approach to suppress the influence of measurement error and noise. The calibration data obtained in 2019 are shown in Figure 4, which are displayed by the azimuth and altitude angle of the dataset. Each data point has a corresponding measured Mueller matrix residual, which will be set as the target value of the ANN model. Each

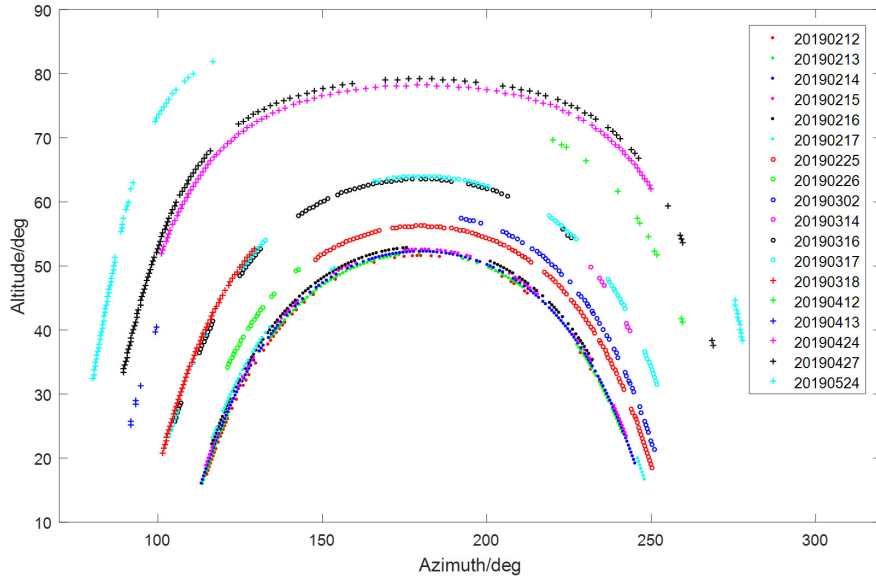


Fig. 4 The calibration data points for ANN model training.

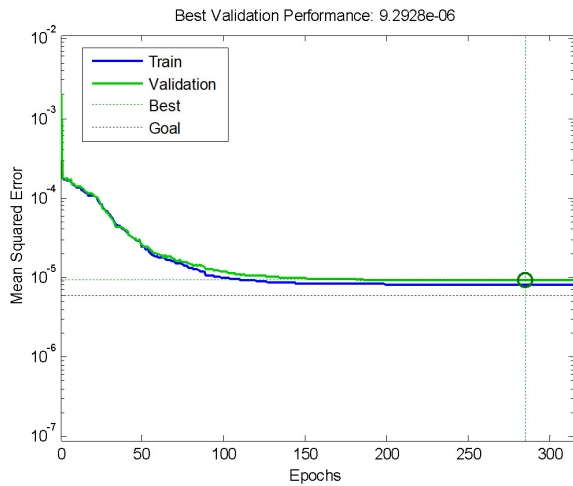


Fig. 5 Loss function of the machine learning model during training.

trajectory with the specified marker in Figure 4 represents the data of the corresponding date.

In order to mitigate the influence of the uneven distribution of the data or the errors in the dataset on the model training, the data are processed with the following three steps:

1. Remove the data points with large measurement errors. Each Mueller matrix measurement of the telescope has six ICU states and eight polarimeter states, thus producing 48 different polarization states. Five frames are acquired to reduce the noise level in each polarization state, and we can get an intensity from each frame. The whole process takes about 53 seconds since 240 intensities are

obtained for each Mueller matrix measurement. Thus, the fluctuation of light intensity caused by weather will induce errors in the measured Mueller matrix, and the data with errors need to be eliminated. The standard deviation of five intensities measured in the same state is used as the criterion to select and eliminate the data affected by light intensity fluctuation, the data with a standard deviation larger than 2% of the mean value of 240 intensities are removed.

2. Remove the data points that experience rapid Mueller matrix change during the measurement. The pointing direction of the telescope changes constantly while tracking the Sun, which results in the time-varying Mueller matrix of the telescope. The maximum value of Mueller matrix change can reach 0.3 per minute at noon in months around the summer solstice. If the change rate of the Mueller matrix is too large, larger than 0.01 per minute, the measured result would deviate from the real value and such data should be removed. According to the physical parametric model, the rate of Mueller matrix change can be derived and used to remove the bad data points.

3. Data equalization. Due to the limitation of observational time, weather, and other factors, the data in Figure 4 is unevenly distributed among azimuth and altitude angles. For example, the data observed from February 12 to February 17 account for 45% of the total data, and all the data distributed in the area with a low altitude angle, which would add to the weight of this area if the data is not equalized. Therefore, the axis of azimuth and altitude angle in Figure 4 are divided evenly by 5

degrees. A maximum number of 15 data points are adopted in each 5×5 grid, and the redundant data points are eliminated to make the dataset as even as possible.

After removing the error data and equalization, the dataset is used for machine learning in the next step. The data from 2019 March 16 and April 24, which account for 15% of the whole dataset, are extracted as the testing dataset of the machine learning model. The remaining 85% of the data are divided randomly by ratio for the training dataset (70%) and validation dataset (15%).

4.2 Training Results

Based on the machine learning model in Section 3 and the processed data in Section 4.1, machine learning training is implemented. Figure 5 shows the relationship between the loss function and the training epoch in the machine learning process. As can be seen from the figure, the loss function dropped rapidly after the training started, and the training process finally stopped because the loss function of the validation dataset did not drop further for 30 consecutive epochs. The smallest MSE in the validation dataset was 9.2928×10^{-6} .

Figure 6 shows the fitting and predictive performance of the ANN model. The left panels provide the relationship between the predicting result of the ANN model and the target value. The target value corresponds to the Mueller matrix residual value for machine learning, and all the matrix elements are displayed in the same plot. If the data point lies on the line of $Y = X$, it means the predictive result equals the training target. The data points are distributed centrally around the line of $Y = X$, and the correlation coefficient is 0.9685 in the training and validation dataset in Figure 6(a). As for the testing dataset in Figure 6(b), the correlation coefficient between the ANN model and the target value is 0.9497, and the data points distribute closely to the line of $Y = X$ as well, which shows the predictive capacity of the ANN model.

The right panels of Figure 6 present the histograms of the Mueller matrix residual and compare the residual distribution before and after the ANN model is involved. The peak-to-valley (PV) value of the residuals in the training and validation dataset is reduced from 0.0891 to 0.0363 after the ANN model is used. In the testing dataset, the PV value is 0.0352 after using the ANN model. Therefore, the performance of the polarization model is considerable when the physical parametric model and the ANN model are combined.

Comparing the histograms in Figure 6, the PV value of the testing dataset is even smaller than that of the training and validation dataset after using the ANN model.

Therefore, the root mean square (RMS) of the deviation is also displayed in the histogram since the PV value could be easily affected by the larger error points.

4.3 Testing Results

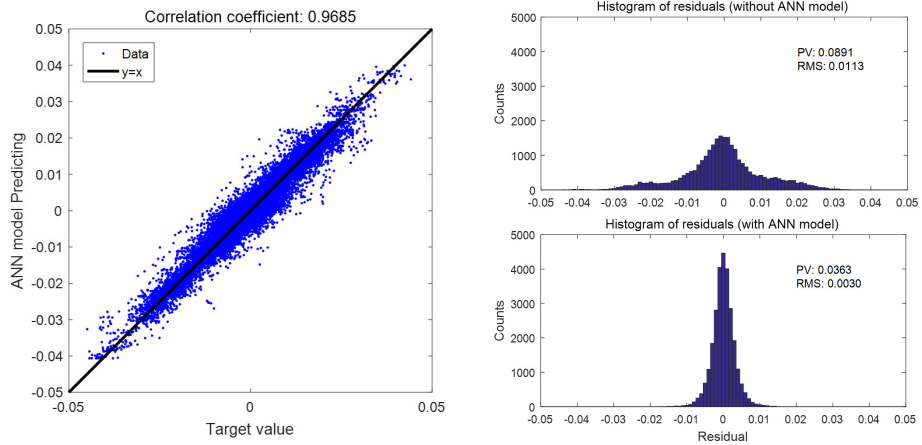
In order to test the predictive capacity of the ANN model further, we examined the performance of the model for each Mueller matrix element in a whole observational day. Figure 7 shows the polarization model residuals of the telescope's Mueller matrix on 2019 April 24, the blue points indicate the residuals of the physical parametric model over time, and the red points represent the residuals after the ANN model is employed. Each subgraph in the figure corresponds to the Mueller matrix element, the horizontal axis indicates the universal time, and the vertical axis shows the residual value of the Mueller matrix. The smaller the deviation of value from 0, the higher the accuracy of the corresponding model.

It can be seen from Figure 7 that the deviation of the residual from 0 is significantly reduced after using the ANN model. In particular, the Mueller matrix elements M_{22} and M_{32} have considerably improved, the maximum deviation drop from about 0.047 to 0.020, other Mueller matrix elements also have significant improvements. The improved model for the M_{23} , M_{24} , M_{32} , M_{34} , M_{42} and M_{43} can effectively reduce the crosstalk among Q, U, and V, and the maximum crosstalk between Q, U, and V is reduced from 0.047 to 0.020. In addition, even though the deviation of M_{21} , M_{31} , M_{41} is smaller than 0.011, the improvements of these elements are extremely important because the I signal of the observational target is generally much larger than the Q, U, and V signals. It can be seen that the data points of these three elements are basically distributed around 0 after using the ANN model. The maximum deviation is about 0.007, which efficiently reduces the influence of crosstalk from I to Q, U, and V.

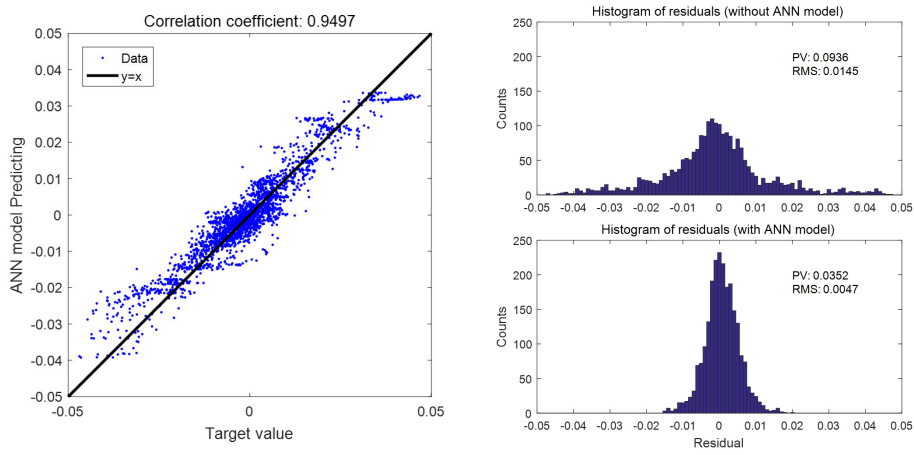
Compared with Figure 2(b), the data gap around 5 o'clock UTC in Figure 7 is due to the eliminated data points in the data preprocessing, since these points experienced rapid Mueller matrix changes during the measurement.

The predictive performance of the ANN model for the testing dataset on 2019 March 16, is shown in Figure 8. The maximum deviation of the Mueller matrix on March 16 is reduced from 0.047 to 0.016, which also achieves great improvement even though the number of the data points is much less than that on 2019 April 24, because of the limited observational time.

The predictive performance in the testing dataset confirms the effectiveness of the ANN model, which can



(a) Training and validation dataset



(b) Testing dataset

Fig. 6 Relationship between the result of the ANN model and the target value.

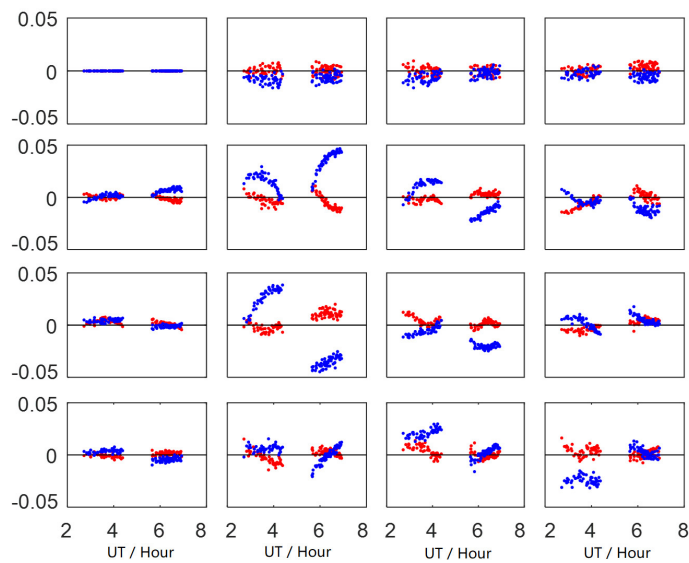


Fig. 7 The Mueller residual of the polarization model on 2019 April 24.

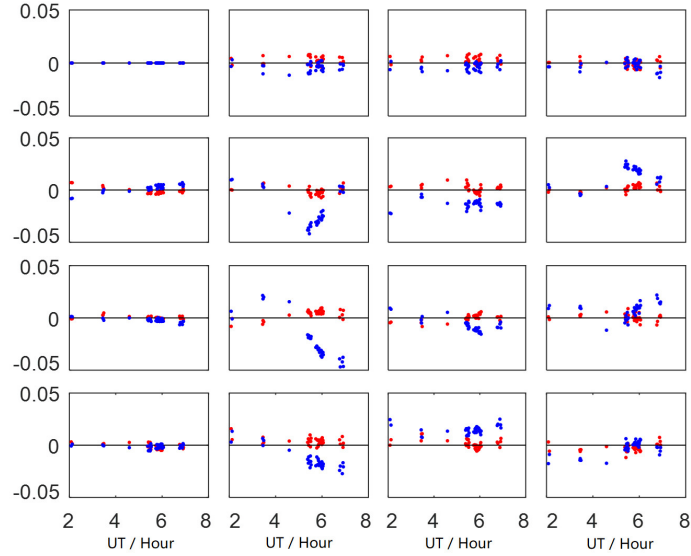


Fig. 8 The Mueller residual of the polarization model on 2019 March 16.

generate the Mueller matrix of the telescope at specific times.

5 CONCLUSIONS AND DISCUSSION

This paper has proposed a new method for polarization modeling of a large ground-based telescope, which involves the physical parametric model and the ANN model. The ANN model, which is a supplement of the physical parametric model, is established based on the relationship between the Mueller matrix residual of the physical parametric model and the pointing direction of the telescope. The combination of the physical parametric model and the ANN model, which is called the compound polarization model, can characterize the polarization property of the telescope very well. The compound polarization model is stable and has high accuracy since it has the advantages of both the physical parametric model and the ANN model.

When training for the ANN polarization model, we have tried deriving the model from the Mueller matrix of the telescope instead of the Mueller matrix residual of the physical parametric model. It was found that the performance of the ANN model derived from the Mueller matrix is as good as that of the ANN residual model in the training dataset, but there may be a large model deviation when the former one was used for predicting the Mueller matrix of the telescope. The ANN model of the Mueller matrix residual is more stable because it is a correction of the physical parametric model, while the ANN model of the Mueller matrix has no physical constraint. Thus, the residual of the physical parametric model is adopted

to build up the ANN model or the compound polarization model in this paper.

The maximum deviation between the polarization model and the measured Mueller matrix of the NVST is reduced from 0.047 to 0.02, which can suppress the crosstalk between the Stokes parameters of the observational targets after polarization correction. In particular, the crosstalk from I to Q, U, and V, which has a higher accuracy requirement, is reduced from 0.011 to less than 0.007.

When setting up the structure of the machine learning model, the results of the multilayer neural network and single-layer neural network have been compared. The residual of the training dataset would decrease when adding the number of network layers or the number of neurons in each layer, but the performance in the testing dataset would not improve further. Especially when the number of hidden layers of the neural network reaches five layers (20 neurons in each layer), the predictive results on the testing dataset become even worse, owing to the overfitting of the data. Therefore, a single hidden layer with 20 neurons is finally employed to build up the ANN model.

Since the accuracy of the ANN model is highly dependent on the training data, the polarization characteristics of the telescope can be properly described only if the data covers all the areas of the azimuth and altitude angle. Thus, it requires a dataset of at least half a year with a time interval of less than a month. In addition, the calibration data in each day is oversampled, which means the sampling intervals can be longer while the time span remains the

same for a whole day. For example, it only takes half an hour to acquire calibration data every 1.5 hours, therefore scientific observations can take place in the rest time.

Acknowledgements We thank the referee for a constructive report. This work was supported by the National Natural Science Foundation of China (Grant Nos. 11833010, 11773069, 11773072, 11873091 and 12073077), Key Research and Development Project of Yunnan Province (202003AD150019), Yunnan Province Basic Research Plan (2019FA001), and the CAS ‘Light of West China’ Program (Y9XB015001).

References

- Ahn, K., & Cao, W. 2019, arXiv e-prints, arXiv:1909.12970
- Anan, T., Huang, Y.-W., Nakatani, Y., et al. 2018, PASJ, 70, 102
- Baron, D. 2019, arXiv e-prints, arXiv:1904.07248
- Beck, C., Schlichenmaier, R., Collados, M., Bellot Rubio, L., & Kentischer, T. 2005a, A&A, 443, 1047
- Beck, C., Schmidt, W., Kentischer, T., & Elmore, D. 2005b, A&A, 437, 1159
- Bettonvil, F. C. M., Collados, M., Feller, A., et al. 2010, in Society of Photo-Optical Instrumentation Engineers (SPIE) Conference Series, 7735, Ground-based and Airborne Instrumentation for Astronomy III, eds. I. S. McLean, S. K. Ramsay, & H. Takami, 77356I
- George, D., & Huerta, E. A. 2018, Physics Letters B, 778, 64
- Guo, J., Bai, X., Deng, Y., et al. 2020, Sol. Phys., 295, 5
- Hála, P. 2014, arXiv e-prints, arXiv:1412.8341
- Hao, Q., Chen, P. F., & Fang, C. 2018, IAU Symposium, 340, 101
- Harrington, D. M., Sueoka, S. R., & White, A. J. 2019, Journal of Astronomical Telescopes, Instruments, and Systems, 5, 038001
- Hofmann, A., Arlt, K., Balthasar, H., et al. 2012, Astronomische Nachrichten, 333, 854
- Hou, J.-F., Xu, Z., Yuan, S., et al. 2020, RAA (Research in Astronomy and Astrophysics), 20, 045
- Huang, X., Wang, H., Xu, L., et al. 2018, ApJ, 856, 7
- Ichimoto, K., Lites, B., Elmore, D., et al. 2008, Sol. Phys., 249, 233
- Kim, E. J., & Brunner, R. J. 2017, MNRAS, 464, 4463
- Liu, W., Yuan, S., & Jin, Z. 2015, Acta Optica Sinica, 35, 328
- Liu, Z., Xu, J., Gu, B.-Z., et al. 2014, RAA (Research in Astronomy and Astrophysics), 14, 705
- Pearson, K. A., Palafox, L., & Griffith, C. A. 2018, MNRAS, 474, 478
- Schou, J., Scherrer, P. H., Bush, R. I., et al. 2012, Sol. Phys., 275, 229
- Skumanich, A., Lites, B. W., Martínez Pillet, V., & Seagraves, P. 1997, ApJS, 110, 357
- Wang, R., Xu, Z., Jin, Z.-Y., et al. 2013, RAA (Research in Astronomy and Astrophysics), 13, 1240
- Xue, Z., Yan, X., Yang, L., et al. 2020, A&A, 633, A121
- Yan, X. L., Yang, L. H., Xue, Z. K., et al. 2018, ApJL, 853, L18
- Yuan, S. 2014, in Astronomical Society of the Pacific Conference Series, 489, Solar Polarization 7, eds. K. N. Nagendra, J. O. Stenflo, Z. Q. Qu, & M. Sampoorna, 297
- Yuan, S. 2019, in Astronomical Society of the Pacific Conference Series, 521, Solar Polarization 8, eds. L. Belluzzi, R. Casini, M. Romoli, & J. T. Bueno